Published in final edited form as:
*J Mol Cell Cardiol*. 2014 September ; 74: 330–339. doi:10.1016/j.yjmcc.2014.06.010.

# Degradation of a Connexin40 mutant linked to atrial fibrillation is accelerated

**Joanna Gemel**[1], **Adria R. Simon**[1,*], **Dakshesh Patel**[2], **Qin Xu**[2], **Arvydas Matiukas**[2], **Richard D. Veenstra**[2,3], and **Eric C. Beyer**[1]

[1]Department of Pediatrics, University of Chicago, Chicago, IL 60637

[2]Department of Pharmacology, SUNY Upstate Medical University, Syracuse, NY 13210

[3]Cell and Developmental Biology, SUNY Upstate Medical University, Syracuse, NY 13210

## Abstract

Several Cx40 mutants have been identified in patients with atrial fibrillation (AF). We have been working to identify physiological or cell biological abnormalities of several these human mutants that might explain how they contribute to disease pathogenesis. Wild type (wt) Cx40 or four different mutants (P88S, G38D, V85I, and L229M) were expressed by transfection of communication-deficient HeLa cells or HL-1 cardiomyocytes. Biophysical channel properties and the sub-cellular localization and protein levels of Cx40 were characterized. Wild type Cx40 and all mutants except P88S formed gap junction plaques and induced significant gap junctional conductances. The functional mutants showed only modest alterations of single channel conductances or gating by trans-junctional voltage as compared to wtCx40. However, immunoblotting indicated that the steady state levels of G38D, V85I, and L229M were reduced relative to wtCx40; most strikingly, G38D was only 20 − 31% of wild type levels. After inhibition of protein synthesis with cycloheximide, G38D (and to a lesser extent the other mutants) disappeared much faster than wtCx40. Treatment with the proteasomal inhibitor, epoxomicin, greatly increased levels of G38D and restored the abundance of gap junctions and the extent of intercellular dye transfer. Thus, G38D, V85I, and L229M are functional mutants of Cx40 with small alterations of physiological properties, but accelerated degradation by the proteasome. These findings suggest a novel mechanism (protein instability) for the pathogenesis of AF due to a connexin mutation and a novel approach to therapy (protease inhibition).



Address correspondence to: Eric C. Beyer M.D., Ph.D., Professor of Pediatrics, University of Chicago, 900 E. 57th St. KCBD 5152, Chicago, IL 60637, Tel: 773-834-1498, FAX: 773-834-1329, ecbeyer@uchicago.edu.
*Present address, School of Medicine, New York University, New York, NY 10016



**Disclosures**
None

**Keywords**

atrial fibrillation; gap junctions; ion channels; connexin40; protein degradation; proteasome

## 1. Introduction

Gap junctions contain intercellular channels (formed of connexins) that allow exchange of ions (and small molecules) between adjacent cells. In the heart, these channels are critical for normal electrical conduction. Abnormalities of connexins have been implicated in both atrial and ventricular arrhythmias.

Atrial fibrillation (AF) is the most common cardiac arrhythmia. It is characterized by a rapid and irregular electrical activation and the loss of atrial muscle contractility. The pathogenesis of AF involves initiating triggers (often rapidly firing ectopic foci located inside the pulmonary veins) and an abnormal atrial tissue substrate that maintains the arrhythmia [1, 2]. It is likely that the abundance and distribution of atrial connexins contribute to that tissue substrate [3].

Two different connexins, Cx40 and Cx43, are abundantly expressed by atrial myocytes and determine the properties of conduction within this tissue [4, 5]. Various alterations of both Cx40 and Cx43 have been observed in patients with AF (reviewed in [6]). The confounding results of these studies may have resulted from the different etiologies and durations of AF in these patients and the extent of failure and structural heart disease. About 15% of AF patients have “lone AF” which develops in apparently normal hearts in the absence of structural abnormalities.

Connexin abnormalities identified in patients with lone AF may help to elucidate the contribution of connexins (and gap junctions) to this disease. Several Cx40 mutants have been identified in patients with lone AF [7, 8]. We have been working to identify any physiological or cell biological abnormalities of these mutants that might help to explain how they contribute to disease pathogenesis. Our general strategy is to express the wild type or mutant Cx40 by transfection of communication-deficient cells and characterize their protein levels, sub-cellular localization, and biophysical channel properties.

In recent studies [9], we concentrated on studying two Cx40 mutants (G38D and M163V). Our electrophysiological experiments showed that these two mutants produced channels with only mildly altered conductance and gating properties when studied individually in transfected N2a cells. However, we found more dramatic alterations when the two mutants were co-expressed, suggesting that they interact with each other. Our new data contrasted with the initial report of G38D [7] which suggested that when expressed, this mutant did not produce a significant level of gap junctional conductance and that cells expressing this mutant showed only very low levels of immunoreactive Cx40 as detected by immunolabeling and microscopy.

In the current study, we have continued cellular/biochemical and physiological characterization of G38D and of several other reported Cx40 mutant proteins associated

with lone AF, including P88S, V85I, and L229M. Our new data confirm that many AF-associated Cx40 mutants make gap junction plaques and functional gap junction channels. The channels may or may not have significant abnormalities. But, most strikingly, our new studies presented here suggest that G38D (and likely some of the other mutants) is unstable as compared to the wild type, and it supports reduced intercellular coupling due to accelerated degradation.

## 2. Material and methods

### 2.1. Connexin-expressing cells

HeLa and N2a cells were cultured as previously described [10, 10, 11]. The mouse HL-1 atrial cardiomyocyte cell line was generated and kindly provided by Dr. W.C. Claycomb (Louisiana State University Medical Center, New Orleans, LA). HL-1 cells were grown in Claycomb medium, supplemented with 10% FBS, 2 mM L-glutamine, 0.1 mM norepinephrine and penicillin/streptomycin 100 U/mL, 100 μg/mL (Sigma, St. Louis, MO) [12]. Human Cx40 DNA was subcloned into the pSFFV-neo or pTracer- CMV2 as described earlier [9]. Mutants of Cx40 containing substitutions: G38D [9], G38E, G38V, G38N, V85I, P88S, and L229M, were generated with the Quick Change Site-Directed Mutagenesis Kit (Agilent Technologies UK, Ltd., Cheshire, UK). The plasmid constructs were purified using the Plasmid Maxiprep Kit (OriGene, Rockville, MD) and the DNA sequences were confirmed to contain only the wanted mutations.

Cells were transiently or stably transfected with connexin DNA using Lipofectamine 2000 for HeLa cells or Lipofectamine 3000 for HL-1 cells (Life Technologies, Grand Island, NY) according to manufacturer's instructions. For immunofluorescence and immunoblot analysis of connexin expression, HeLa cells were transiently transfected with constructs in pSFFV-neo. For the initial assessment of the stability of mutant proteins in comparison to a wild type Cx40, HeLa cells were transiently transfected with connexin DNAs in pTracer-CMV2. For the electrophysiological experiments, N2a cells were transiently transfected with connexin DNAs in pTracer-CMV2.

For the cycloheximide experiments and experiments with inhibitors of protein degradation HeLa cells stably transfected with pSFFV-neo constructs were used. Stable clones were selected by culturing in medium containing G418 (1000 μg/mL) (Life Technologies). Clones were screened for Cx40 expression by immunofluorescence with anti-connexin antibodies.

### 2.2. Cell treatments

Hela cells expressing wild type or mutant Cx40 were treated with 40 μg/mL cycloheximide (EMD Millipore, Billerica, MA) for 0, 1, 3, 6 or 24 hours or with 0.5μM epoxomicin (Calbiochem-Novabiochem Corp.) [13], 0.1mM chloroquine (Sigma, St. Louis, MO) [14], 5 mM3-methyl adenine (3-MA, EMD Millipore, Billerica, MA) or DMSO (used as a solvent for stock solutions of epoxomicin or cycloheximide) for 18 hours.

At the end of treatments cells were harvested for immunoblot analysis which was performed as described below.

### 2.3 Analysis of protein ubiquitination

Hela cells expressing wild type Cx40 or G38D were treated with 0.5μM epoxomicin or DMSO alone for 18 h, harvested in PBS containing protease inhibitors [5], and centrifuged at 150g for 7 min. Pelleted cells were resuspended in the same buffer, then disrupted by repeated passage through 20 and 27 gauge needles. Ubiquitinated proteins were isolated from the lysate using the UbiQaptureTM-Q Kit (Enzo Life Sciences, Farmingdale, NY) according to manufacturer instructions with binding of proteins to the UbiQaptureTM-Q matrix beads over 4 h. Following washing, bound material was analyzed by immunoblotting.

### 2.4. Antibodies

Cx40 was detected using rabbit polyclonal antibodies directed against the carboxy-terminal domain of Cx40 (cat. no 36–4900 Life Technologies) at 1:250 dilution for all immunofluorescence and at 1:1000 dilution for most immunoblotting experiments. For blots of HL-1 cells and of ubiquitinated proteins, Cx40 was detected using goat polyclonal antibodies directed against the carboxy-terminal domain of Cx40 (cat. no sc-20499, Santa Cruz Biotechnology, Inc., Santa Cruz, CA). Mouse monoclonal anti-GFP antibodies were obtained from Life Technologies (cat. no 33–2600) and used at a 1:250 dilution for immunoblotting. Mouse monoclonal anti-β-tubulin antibodies were obtained from Sigma (cat. no T5283) and were used at 1:2000 dilution for immunoblotting. Mouse monoclonal anti-β-actin antibodies were obtained from Sigma (cat. no A2228) and were used at 1:2000 dilution for immunoblotting. Cy3-conjugated goat anti-rabbit IgG and HRP-conjugated goat anti-rabbit or anti-mouse IgG antibodies were obtained from Jackson ImmunoResearch (West Grove, PA). HRP-conjugated donkey anti-goat IgG antibodies were obtained Santa Cruz Biotechnology, Inc. The ubiquitin-conjugate specific HRP-linked antibody from the UbiQaptureTM-Q Kit was used at a 1:1000 dilution.

### 2.5. Immunoblot Analysis

Cell homogenates were prepared 48 h after transfection with connexin DNA as described by Gong et al. [15]. Immunoblots were performed as described earlier [5]. The protein concentrations of homogenates were determined using the method of Bradford (1976) (Bio-Rad, Richmond, CA)[16]. Aliquots containing 20 μg of protein were separated by SDS-PAGE on 10% polyacrylamide gels and blotted onto Immobilon-P membranes (Millipore, Bedford, MA). ProSieve QuadColor Protein Markers (Lonza Walkersville, Inc., Walkersville, MD) were used to calibrate the gels. Depending on the desired sensitivity, immunoblots were developed with ECL, ECL Prime (GE Healthcare Biosciences) or SuperSignal WestFemto Chemiluminescence reagents (Thermo Fisher Scientific Inc., Rockford, IL) and exposure to X-ray film. Final figures for publication were assembled by cutting and cropping to include representative examples and to juxtapose panels to facilitate comparisons.

### 2.6. Immunofluorescence analysis of connexin expression

For microscopy, cells were cultured on multi-well slides. Cells were fixed in methanol/acetone (1:1) for 2 minutes. 27 hours after transfection with connexin DNAs and stained as previously described [11]. Cells were studied using the 40X Plan Apochromat objective in

an Axioplan 2 microscope (Carl Zeiss Meditec, Munich, Germany). Images were captured with a Zeiss Axiocam digital camera using Zeiss AxioVision software.

### 2.7. Intercellular transfer of propidium iodide

For intercellular transfer of microinjected propidium iodide (PI) HeLa cells were cultured on glass coverslips and transiently transfected with Cx40 (or mutant) DNA in pTracer-CMV2. 24 hours after transfections cells were treated for 4 hours with 0.5μM epoxomicin (Calbiochem-Novabiochem) or DMSO (used as a solvent for stock solutions of epoxomicin). For injections, cover slips were transferred to F-12 media (Life Technologies) buffered with 15 mM HEPES. An individual cell in the middle of a cluster of ∼5 cells expressing green fluorescent protein (GFP) was injected with 2 mg/mL propidium iodide (Life Technologies). Cell-to-cell coupling was quantified by counting the number of cells that showed red fluorescent staining 5 min after injection. The statistical significance of differences between treated and untreated cells was calculated using Student's t-test.

### 2.8. Gap junction conductance measurements

Dual whole cell patch clamp experiments were performed using conventional 140 mM NaCl or KCl bath saline or patch electrode solutions and junctional conductance-voltage curves were corrected for series resistance errors as previously published [9, 17]. Steady-state $g_j$ – $V_j$ relationships were normalized by dividing $g_j$ by the linear slope $g_j$ ($g_{max}$) value for each experiment ($G_j = g_j/g_{j,max}$) and fitting each voltage polarity of the $G_j$ -$V_j$ curve with the typical two state Boltzmann equation as previously described [17, 18]. Fitted curves were calculated using Clampfit software (Molecular Devices) using the sum of squared errors minimization procedure, and graphs were prepared using Origin7.5 or 8.6. Gap junction channel conductances ($\gamma_j$) were determined from the linear regression fit of a channel current amplitude – voltage relationship ranging from ±10 to ±50 mV. Channel current amplitudes were measured from Gaussian fits of all points histograms derived from low pass filtered gap junction channel recordings for each 30 sec $V_j$ pulse as previously described [9, 19].

## 3. Results

### 3.1. Many AF-associated Cx40 mutants make gap junction plaques and functional gap junction channels

To examine the cellular trafficking of Cx40 mutants, we transiently transfected communication-deficient HeLa cells with wt Cx40 or several of the AF-associated mutants and determined the localization of immunoreactive Cx40 by immunofluorescence microscopy (Fig. 1). As expected, wtCx40 was localized in a punctuate distribution along appositional membranes within the cytoplasm (in reticular and/or peri-nuclear distributions). This localization likely represents connexins within gap junction plaques and within the biosynthetic pathway. Most of the Cx40 mutants, including G38D, V85I, and L229M, exhibited similar distributions to wtCx40 suggesting that these proteins also followed reasonably normal trafficking pathways and made gap junctions. There were mild variations in the size and abundance of gap junctions, with a suggestion of reductions for G38D. Only P88S differed dramatically from the others; all immunoreactive Cx40 was found intracellularly in HeLa cells transfected with this mutant. To determine the site of retention

of the P88S mutant, we reacted transiently transfected cells with antibodies directed against PDI, a marker of the endoplasmic reticulum or against Golgi-58K protein, a marker of the Golgi apparatus (not shown). There was little overlap between Cx40 and PDI immunoreactivities. However, there was significant colocalization of the P88S mutant and the 58K protein. These observations suggest that P88S was retained intracellularly in the Golgi apparatus and did not form gap junctions.

We also transiently transfected N2a cells with the mutants and studied the properties of the induced gap junctions using the double whole cell patch clamp technique. Both wtCx40 and G38D induced significant gap junctional conductances (as previously reported) [9]. P88S did not induce conductances that were significantly greater than those of untransfected cells (data not shown). Therefore, since P88S appears to be a loss-of-function mutant with impaired trafficking, it was not studied further. Our data regarding P88S are similar to the observations made in the original characterization of this mutant [7] and in studies of mutations of other connexins at this position [13, 20].

The two other Cx40 mutants (V85I and L229M) both produced significant gap junctional conductances in N2a cell pairs (7.4±3.7 and 3.2±0.5 nS, respectively as compared to 4.8±1.3 nS for wtCx40; mean ± SEM, n=6 pairs for all constructs). The properties of gating by transjunctional voltage ($V_j$) were also assessed for each of these mutants. Fig. 2A shows graphs of normalized junctional conductance, $G_j$, vs. $V_j$, and the parameters of the fits of these data to a Boltzmann equation are shown in supplementary Table 1 V85I produced gap junctions that exhibited a minimally different $V_j$-dependence from those of wtCx40. L229M gap junctions were somewhat more sensitive to $V_j$ than wild type Cx40 (with $V_{1/2}$ −37 and +38 mV) and showed reduced minimal (residual) conductances ($G_{j,min}$ 0.10 and 0.11 for negative and positive polarities) as compared to wtCx40 ($G_{j,min}$ 0.16, 0.20).

When we were able to obtain and study poorly coupled cell pairs, we determined the conductances of single channels ($\gamma_j$) composed of the different Cx40 mutants (Fig. 2B–E). Wild type Cx40 channels had a $\gamma_j$ of 149 ± 2 pS (which compares well to the previous determinations of (rodent and human) Cx40 channels [19, 21]. As previously reported, G38D channels had an increased $\gamma_j$ of 178 ± 2 pS [9]. The $\gamma_j$ of L229M (148 ± 2 pS) was not different from wtCx40 and that of V85I was increased to 159 ± 2 pS.

### 3.2. A Cx40 mutant has reduced abundance and stability

We sought to identify an alternative explanation for abnormalities conferred by Cx40 mutations that caused rather modest alterations of function. One clue was the difficulty of the original authors in detecting gap junctions formed of G38D [7] and our own data suggesting that this mutant made somewhat smaller or less frequent gap junctions than the wild type protein (Fig. 1). We considered that at least some of the mutants might have reduced levels or stabilities.

In order to compare steady state levels of wtCx40 and the mutants by immunoblotting, we analyzed replicate transient transfections of constructs that only differed according to the point mutations using the vector pTracer-CMV2 (which also drives expression of GFP allowing us to correct for any differences in the efficiency of transfection by loading

identical amounts of cell lysates and blotting for GFP as well as Cx40). We initially performed this study in HeLa cells (Fig. 3A,B). Blotting of all homogenates with an antibody to β-tubulin showed that loading was relatively uniform. In transfected cells, wtCx40 protein was abundant and was easily detected. Each of the AF-associated mutants was also detected, but their levels were less than those of wtCx40. L229M was present at ∼75% of the levels of wtCx40; V85I was reduced to ∼33%; and G38D was reduced to ∼20%. These data suggested the possibility that these Cx40 mutants were less stable than the wtCx40.

To test whether similar differences also occurred in cardiac myocytes, we preformed similar experiments using mouse atrial derived HL-1 cardiomyocytes which have been extensively used for *in vitro* studies of cardiac biology [22]. Although these cells express low endogenous levels of Cx40 (not shown), transfection produced such substantial levels of Cx40 that it was not visible in a comparable exposure of an immunoblot of untransfected cells (Fig. 3C). In transfected HL-1 cells, wtCx40 protein was abundant and was present at much greater levels than any of the AF-associated mutants (Fig. 3 C,D). G38D was reduced to 31% of wild type levels, V85I was reduced to 33%, and L229M was reduced to 51%. Thus, the mutants showed similar effects regardless of the cell line in which they were expressed .

We investigated the stability of wtCx40 and these mutants by incubating stably transfected HeLa cells with cycloheximide in order to inhibit *de novo* protein synthesis followed by immunodetection after 1–24 hours of treatment (Fig. 3 E,F). Similar to the half-lives determined for other wild type connexins [23, 24], wtCx40 gradually disappeared over the course of the experiment such that about half was gone after several hours, and the protein was very dramatically reduced (although still detectable) after 24 h. G38D was most dramatically different: its levels were reduced by ∼90% within 3 h. V85I showed a disappearance that was intermediate between G38D and wtCx40. L229M was degraded only a little faster than wtCx40.

### 3.3. G38D is degraded by the proteasome, and proteasomal inhibition restores function

Previous studies by our group and others have established roles for several cellular systems in the degradation of connexins, including the proteasome, the lysosome and the autophagosome [14, 25–29]. Therefore, to identify proteolytic pathways that were important for the accelerated degradation of G38D, we transiently transfected HeLa cells with wtCx40 or G38D, treated them with inhibitors of these different activities (for 18 h), and determined the levels of immunoreactive Cx40 by immunoblotting (Fig. 4). As anticipated (based on the involvement of all three systems in the degradation of wild type connexins), treatment with epoxomicin, chloroquine, or 3-methyladenine all led to moderate increases (2–3 fold) in the levels of wtCx40. The increases of G38D in cells treated with chloroquine or 3-MA were of similar magnitude, suggesting that lysosomal and autophagosomal degradation had rather similar impacts on both wt and mutant connexin. In contrast, epoxomicin lead to a huge increase in G38D (Fig.4). In multiple independent experiments (n=4), the increase was 8.0 ± 1.0 fold. This suggested that the proteasome was responsible for the accelerated degradation of this mutant. We also tested the panel of inhibitors on cells transfected with V85I or

L229M; consistent with their longer half-lives, each drug led to moderate increases in immunoreactive connexin (data not shown), but the enhancement with proteasomal inhibition was less dramatic than for G38D (<2.5-fold) similar to the results obtained with wtCx40.

Based on its ability to slow the degradation of G38D, we also tested the effects of epoxomicin on the abundance of gap junction plaques and on intercellular communication in cells expressing this mutant. Epoxomicin treatment for 4 h had little detectable effect on the distribution of immunoreactive Cx40 or on the extent of transfer of micro-injected propidium iodide in cells expressing wtCx40 (Fig. 5). Epoxomicin appeared to increase the size and frequency of gap junctions between cells expressing G38D (Fig. 5 A). But, most importantly, epoxomicin dramatically increased the extent of transfer of a microinjected tracer in cells expressing this mutant. In control cultures of cells transiently transfected with G38D, propidium transfer was only observed in ∼50% of injections (n=29) and it only transferred to 1.7±0.3 neighboring cells; in contrast, following treatment with epoxomicin for 4 h, dye transfer was observed in 100% of injections (n=12) and was detected in 4.3± 0.3 neighboring cells (Fig. 5 B). Epoxomicin treatment of the G38D–expressing cells restored transfer of this tracer to a level similar to that in untreated or treated cells expressing wtCx40.

### 3.4. Cx40 and G38D are ubiquitinated

Proteasomal degradation of many proteins follows covalent attachment of ubiquitin. Therefore, we examined whether wtCx40 and G38D were ubiquitinated and whether this modification was enhanced by proteasomal inhibition. We prepared lysates from stably transfected HeLa cells, isolated ubiquitinated proteins, and analyzed them by immunoblotting (Fig. 6). Blotting with anti-ubiquitin antibodies showed that untreated cell lines expressing either wtCx40 or G38D contained few ubiquitinated proteins (visible only with a long blot exposure), but many more were detected following epoxomicin treatment (Fig. 6A,C). Following epoxomicin treatment the abundance and diversity of ubiquitinated proteins was hugely increased similarly in cells expressing either wtCx40 or G38D (Fig. 6 A,C). The identical blot was stripped and probed with anti-Cx40 antibodies (Fig. 6 C, D). A short exposure of the blot shows that immunoreactive bands of ∼40 kDa were present were isolated with the ubiquitinated proteins from cells expressing both wtCx40 and G38D. A longer exposure of the blot (Fig. 6B) reveals high molecular weight immunoreactive bands, likely representing polyubiquitinated form of both wtCx40 and G8D. Moreover, the abundance of these slower migrating forms was increased following proteasomal inhibition with epoxomicin.

### 3.5. AF Cx40 mutants also affect co-expressed wild type Cx40

We hypothesized that the mutants might exert “dominant-negative” effects on wtCx40, since the affected patients are not homozygous for these mutants. They carry either somatic or heterozygous germline mutations. Therefore, we examined the possible interactions of each mutant with co-expressed wtCx40 by determining the levels of total immunoreactive Cx40 in cells co-transfected with wtCx40 and an equal amount of plasmid encoding wtCx40 or a mutant (G38D, V85I, or L229M) (Fig. 7). In each case, the total Cx40 levels were lower in

cells co-transfected with a mutant than for cells transfected with a “double dose” of wtCx40, suggesting that the mutants also accelerated the degradation of the wild type protein. The reductions of total Cx40 levels paralleled the reductions of levels of each mutant when expressed alone.

### 3.6. Amino acid substitutions show different requirements at position 38

To further clarify the importance of the residue at position 38, we generated several site-directed mutants in which the glycine was replaced with different residues. We chose to substitute glutamate (G38E), because it would make the same negative charge substitution as aspartate; valine (G38V), because it would be a similar sized, but non-polar substitution, or asparagine (G38N), because it would be a similarly shaped amino acid substitution but without the negative charge. Following transient transfection of HeLa cells with each of these constructs, immunofluorescence was performed and showed that each of these three mutants localized to appositional membranes implying that they formed gap junction plaques (Fig.8A). Immunoblotting was also performed, and it showed that each of these mutants had similar levels to wtCx40 (Fig. 8B).Only G38D was reduced, suggesting that the aspartate substitution uniquely reduced Cx40 stability.

We also studied the electrophysiological properties of these three substitution mutants using the double whole cell patch clamp technique. All of the N2a cell pairs transiently expressing the G38E or G38N mutant proteins were robustly coupled while none of the G38V expressing cells exhibited functional coupling (Fig. 8C). We did observe one poorly coupled (0.1 nS) G38N cell pair with channels of reduced size (112 ± 16 pS, Fig. 8D,E).

## 4. Discussion

In the current study, we continued our investigations of the Cx40 mutant, G38D, and studied other Cx40 mutants linked to AF (including V85I and L229M). The electrophysiological data presented in our previous study [9] and in the current one show that these three mutants all efficiently form gap junction channels and that their unitary conductances and $V_j$-dependent gating properties are only mildly different from those of wtCx40. It is uncertain that any of these electrophysiological abnormalities would significantly affect conduction within the atrium.

However, we did observe that levels of all three of these mutants were reduced when expressed in transfected cells and that they disappeared more rapidly than wtCx40 when ongoing protein synthesis was blocked. These observations suggested that each of these proteins was relatively unstable. Indeed, a co-expression experiment (Fig. 6) suggested that these mutants could also accelerate the degradation of accompanying wtCx40. Altered levels of Cx40 (and possibly an altered Cx40:Cx43 ratio) can certainly alter the conduction among atrial myocytes [30]. Because of various experimental advantages, many of our experiments were performed using a transformed cancer cell line (HeLa) in which connexins are not subjected to continuous electrical activity or mechanical stresses as they would be in the heart. However, the similar results that we obtained using HL-1 cardiac myocytes give confidence that our findings should also apply in hearts of individuals expressing these mutations.

Because G38D showed the most dramatic differences from the wild type protein, it was investigated most thoroughly. We observed that treatment of G38D–expressing cells with a proteasomal inhibitor (epoxomicin) restored levels of the protein, its abundance at appositional membranes (gap junctional plaques), and the level of intercellular coupling. This represents a rather novel observation that connexin mutants may lead to disease through “loss of function” due to increased proteasomal degradation of the mutant protein. We suspect that the Cx40 protein is partially mis-folded or is slow to assume its proper folding, therefore it is susceptible to “quality control”. Our findings regarding these Cx40 mutants parallel the conclusions drawn from our recent studies of a Cx50 frame-shift mutant containing an abnormal carboxyl-terminus that increases its susceptibility to the proteasome [31].

Some, but not all, of the structural bases of our observed abnormalities are interpretable. The three Cx40 mutants studied here all alter amino acids within transmembrane domains; perhaps they alter packing of the helices. It is not surprising that substitution of a negatively charged residue (aspartate) for glycine-38 (in the middle of the first transmembrane domain) might alter the structure of Cx40 and its formation of connexons and channels, leading to instability. However, our site directed-mutagenesis studies have shown that the accelerated proteasomal degradation is specifically impaired by the aspartate substitution (even the negatively charged residue, glutamate, did not have this effect). Moreover, the identity of the residue at position 38 is important in determining other properties, as shown by the loss of function caused by the valine substitution and the change in unitary conductance caused by the asparagine. Valine-85 is located in the middle of transmembrane domain 2; it might have been predicted that a substitution of isoleucine (similar size and also hydrophobic) would not have been consequential. Leucine-229 is located at the end of the fourth transmembrane domain; methionine would have some differences in shape and interactions with adjacent residues due to the sulfur-containing side chain and less hydrophobicity.

The ubiquitin-proteasome system has previously been implicated in the ER-associated degradation of wild type and mutant connexins [25, 31–33]. The simplest explanation for the faster degradation of G38D is that most of the protein undergoes proteasomal degradation before it can reach the plasma membrane and form gap junction plaques (probably in early compartments of the secretory pathway). Some Cx32 mutants associated with X-linked Charcot-Marie-Tooth disease undergo retro-translocation to the ER prior to proteasomal degradation [32]. Many proteins are targeted for proteasomal degradation by enzymatic modification with ubiquitin chains. Our blots suggest that both wt Cx40 and G38D are susceptible to polyubiquitination and that this modification is more prominent for the mutant (Fig. 6). However, much of the wtCx40 and G38D isolated using an anti-ubiquitin matrix appears unmodified (Fig. 6D). It may be that many unmodified subunits are associated with the ubiquitinated Cx40 or that some of the modification was lost in our sample processing.

Our findings suggest a potential therapeutic approach to treating some cases of AF (and other diseases) caused by connexin mutants: prevention of degradation. Previous studies have suggested that disruptions of proteostasis (the homeostasis of protein production, function, and degradation) is involved in the electrical remodeling that provides the substrate for atrial fibrillation [34]. A component of these derangements is proteolysis [35, 36].

Proteasomal inhibitors (like bortezomib) are currently being used to treat patients with multiple myeloma and other hematologic malignancies [37, 38]. Proteasomal inhibitors may have utility in some acute cardiac events (like ischemia- reperfusion injury) where over-activity of the ubiquitin-proteasome system contributes to the injury [39]. However, case reports show that these agents sometimes cause cardiac toxicities [40]. This is not surprising, since proteasomal dysfunction has been implicated in various chronic cardiac pathologies (such as cardiomyopathies and heart failure), leading to accumulation of polyubiquitinated proteins and proteotoxicity [41, 42]. Thus, it is likely that global proteasomal inhibition might produce much more harm than good [41].

However, there may be appropriate strategies for more selective intervention. Ubiquitination of proteins targeted for degradation is accomplished by a series of enzymes (E1, E2, and E3); the E3 ligases (alone or in combination with the E2 enzymes) provide substrate specificity. While the enzymes that specifically lead to the modification (and degradation) of Cx40 are not yet known, they are being identified for other connexins [43, 44]. Thus, it may eventually be possible to improve Cx40 function by specifically reducing its proteasomal degradation. Interventions that improved folding of mutant connexins and consequently decreased their proteolysis might be an alternative therapy. Chaperones that associate with connexins are being identified [45], and trafficking of some mutant connexins is improved by chemical or temperature treatments that facilitate folding [13, 46]. Electrical, contractile, and structural remodeling of cardiac myocytes is prevented by increased expression of heat shock proteins attenuating the substrate for atrial fibrillation [34]. Since a brief heat stress can prevent connexin degradation in cultured myocytes [47], it seems possible that heat shock proteins could act as molecular chaperones for cardiac connexins.

## Supplementary Material

Refer to Web version on PubMed Central for supplementary material.

## Acknowledgments

This work was supported by grants from the National Institutes of Health: HL59199 (to ECB and RDV) and HL042220 (to RDV).

## Abbreviations

| | |
|---|---|
| **AF** | atrial fibrillation |
| **Cx** | connexin |
| **DMSO** | dimethyl sulfoxide |
| **GFP** | green fluorescent protein |
| $\mathbf{g_j}$ | junctional conductance |
| $\mathbf{G_j}$ | normalized junctional conductance |
| $\mathbf{G_{j,max}}$ | maximum junctional conductance |
| $\mathbf{G_{j,min}}$ | minimum junctional conductance |

| | |
|---|---|
| **HEPES** | 4-(2-hydroxyethyl)-1-piperazineethanesulfonic acid |
| **$I_j$** | junctional current |
| **3-MA** | 3-methyl adenine |
| **PDI** | protein disulfide isomerase |
| **PI** | propidium iodide |
| **SDS-PAGE** | Sodium Dodecyl Sulfate Polyacrylamide Gel Electrophoresis |
| **q** | electron equivalents |
| **wt** | wild type |
| **$V_{½}$** | half-inactivation voltage |
| **$V_j$** | transjunctional voltage |
| **$V_m$** | membrane potential |
| **z** | gating charge valence |
| **$\gamma_j$** | gap junction channel conductance |

## Reference List


1. Allessie MA, Boyden PA, Camm AJ, Kleber AG, Lab MJ, Legato MJ, et al. Pathophysiology and prevention of atrial fibrillation. Circulation. 2001; 103:769–777. [PubMed: 11156892]
2. Iwasaki YK, Nishida K, Kato T, Nattel S. Atrial fibrillation pathophysiology: implications for management. Circulation. 2011; 124:2264–2274. [PubMed: 22083148]
3. Spach MS, Starmer CF. Altering the topology of gap junctions a major therapeutic target for atrial fibrillation. Cardiovasc Res. 1995; 30:337–344. [PubMed: 7585823]
4. Saffitz JE, Kanter HL, Green KG, Tolley TK, Beyer EC. Tissue-specific determinants of anisotropic conduction velocity in canine atrial and ventricular myocardium. Circ Res. 1994; 74:1065–1070. [PubMed: 8187276]
5. Lin X, Gemel J, Glass A, Zemlin CW, Beyer EC, Veenstra RD. Connexin40 and connexin43 determine gating properties of atrial gap junction channels. J Mol Cell Cardiol. 2010; 48:238–245. [PubMed: 19486903]
6. Kato T, Iwasaki YK, Nattel S. Connexins and atrial fibrillation: filling in the gaps. Circulation. 2012; 125:203–206. [PubMed: 22158757]
7. Gollob MH, Jones DL, Krahn AD, Danis L, Gong XQ, Shao Q, et al. Somatic mutations in the connexin 40 gene (*GJA5*) in atrial fibrillation. N Engl J Med. 2006; 354:2677–2688. [PubMed: 16790700]
8. Yang Y-Q, Liu X, Zhang XL, Wang XH, Tan HW, Shi HF, et al. Novel connexin40 missense mutations in patients with familial atrial fibrillation. Europace. 2010; 12:1421–1427. [PubMed: 20650941]
9. Patel D, Gemel J, Xu Q, Simon AR, Lin X, Matiukas A, et al. Atrial fibrillation-associated Connexin40 mutants make hemichannels and synergistically form gap junction channels with novel properties. FEBS Lett. 2014; 588:1458–1464. [PubMed: 24457199]
10. Veenstra RD, Wang HZ, Westphale EM, Beyer EC. Multiple connexins confer distinct regulatory and conductance properties of gap junctions in developing heart. Circ Res. 1992; 71:1277–1283. [PubMed: 1382884]
11. Gemel J, Valiunas V, Brink PR, Beyer EC. Connexin43 and connexin26 form gap junctions, but not heteromeric channels in co-expressing cells. J Cell Sci. 2004; 117:2469–2480. [PubMed: 15128867]

12. Claycomb WC, Lanson NAJ, Stallworth BS, Egeland DB, Delcarpio JB, Bahinski A, et al. HL-1 cells: a cardiac muscle cell line that contracts and retains phenotypic characteristics of the adult cardiomyocyte. Proc Natl Acad Sci U S A. 1998; 95:2979–2984. [PubMed: 9501201]
13. Berthoud VM, Minogue PJ, Guo J, Williamson EK, Xu X, Ebihara L, et al. Loss of function and impaired degradation of a cataract-associated mutant connexin50. Eur J Cell Biol. 2003; 82:209–221. [PubMed: 12800976]
14. Lichtenstein A, Minogue PJ, Beyer EC, Berthoud VM. Autophagy: a pathway that contributes to connexin degradation. J Cell Sci. 2011; 124:910–920. [PubMed: 21378309]
15. Gong XQ, Shao Q, Lounsbury CS, Bai D, Laird DW. Functional characterization of a GJA1 frameshift mutation causing oculodentodigital dysplasia and palmoplantar keratoderma. J Biol Chem. 2006; 281:31801–31811. [PubMed: 16891658]
16. Bradford MM. A rapid and sensitive method for the quantitation of microgram quantities of protein using the principle of protein-dye binding. Anal Biochem. 1976; 72:248–254. [PubMed: 942051]
17. Veenstra RD. Voltage clamp limitations of dual whole-cell gap junction current and voltage recordings. I Conductance measurements. Biophys J. 2001; 80:2231–2247. [PubMed: 11325726]
18. Spray DC, Harris AL, Bennett MV. Equilibrium properties of a voltage-dependent junctional conductance. J Gen Physiol. 1981; 77:77–93. [PubMed: 6259274]
19. Lin X, Fenn E, Veenstra RD. An amino-terminal lysine residue of rat connexin40 that is required for spermine block. J Physiol. 2006; 570:251–269. [PubMed: 16284078]
20. Pal JD, Berthoud VM, Beyer EC, Mackay D, Shiels A, Ebihara L. Molecular mechanism underlying a Cx50-linked congenital cataract. Am J Physiol Cell Physiol. 1999; 276:C1443–C1446.
21. Beblo DA, Wang HZ, Beyer EC, Westphale EM, Veenstra RD. Unique conductance, gating, and selective permeability properties of gap junction channels formed by connexin40. Circ Res. 1995; 77:813–822. [PubMed: 7554128]
22. White SM, Constantin PE, Claycomb WC. Cardiac physiology at the cellular level: use of cultured HL-1 cardiomyocytes for studies of cardiac muscle cell structure and function. Am J Physiol Heart Circ Physiol. 2004; 286:H823–H829. [PubMed: 14766671]
23. Musil LS, Goodenough DA. Biochemical analysis of connexin43 intracellular transport, phosphorylation, and assembly into gap junctional plaques. J Cell Biol. 1991; 115:1357–1374. [PubMed: 1659577]
24. Berthoud VM, Minogue PJ, Laing JG, Beyer EC. Pathways of connexin and gap junction degradation. Cardiovasc Res. 2004; 62:256–267. [PubMed: 15094346]
25. Laing JG, Beyer EC. The gap junction protein connexin43 is degraded via the ubiquitin proteasome pathway. J Biol Chem. 1995; 270:26399–26403. [PubMed: 7592854]
26. Laing JG, Tadros PN, Westphale EM, Beyer EC. Degradation of connexin43 gap junctions involves both the proteasome and the lysosome. Exp Cell Res. 1997; 236:482–492. [PubMed: 9367633]
27. Qin H, Shao Q, Igdoura SA, Alaoui-Jamali MA, Laird DW. Lysosomal and proteasomal degradation play distinct roles in the life cycle of Cx43 in gap junctional intercellular communication-deficient and -competent breast tumor cells. J Biol Chem. 2003; 278:30005–30014. [PubMed: 12767974]
28. VanSlyke JK, Musil LS. Cytosolic stress reduces degradation of connexin43 internalized from the cell surface and enhances gap junction formation and function. Mol Biol Cell. 2005; 16:5247–5257. [PubMed: 16135529]
29. Kjenseth A, Fykerud T, Rivedal E, Leithe E. Regulation of gap junction intercellular communication by the ubiquitin system. Cell Signal. 2010; 22:1267–1273. [PubMed: 20206687]
30. Beauchamp P, Yamada KA, Baertschi AJ, Green K, Kanter EM, Saffitz JE, et al. Relative contributions of connexins 40 and 43 to atrial impulse propagation in synthetic strands of neonatal and fetal murine cardiomyocytes. Circ Res. 2006; 99:1216–1224. [PubMed: 17053190]
31. Minogue PJ, Beyer EC, Berthoud VM. A connexin50 mutant, CX50fs, that causes cataracts is unstable, but is rescued by a proteasomal inhibitor. J Biol Chem. 2013; 288:20427–20434. [PubMed: 23720739]

32. VanSlyke JK, Deschenes SM, Musil LS. Intracellular transport, assembly, and degradation of wild-type and disease-linked mutant gap junction proteins. Mol Biol Cell. 2000; 11:1933–1946. [PubMed: 10848620]
33. Sakaguchi H, Yamashita S, Miura A, Hirahara T, Kimura E, Maeda Y, et al. A novel GJB1 frameshift mutation produces a transient CNS symptom of X-linked Charcot-Marie-Tooth disease. J Neurol. 2011; 258:284–290. [PubMed: 20857133]
34. Meijering RA, Zhang D, Hoogstra-Berends F, Henning RH, Brundel BJ. Loss of proteostatic control as a substrate for atrial fibrillation: a novel target for upstream therapy by heat shock proteins. Front Physiol. 2012; 3:36. [PubMed: 22375124]
35. Brundel BJJM, Henning RH, Kampinga HH, Van Gelder IC, Crijns HJGM. Molecular mechanisms of remodeling in human atrial fibrillation. Cardiovasc Res. 2002; 54:315–324. [PubMed: 12062337]
36. Brundel BJJM, Ausma J, Van Gelder IC, Van Der Want JJL, van Gilst WH, Crijns HJGM, et al. Activation of proteolysis by calpains and structural changes in human paroxysmal and persistent atrial fibrillation. Cardiovasc Res. 2002; 54:380–389. [PubMed: 12062342]
37. Chauhan D, Hideshima T, Anderson KC. Proteasome inhibition in multiple myeloma: therapeutic implication. Ann Rev Pharmacol Toxicol. 2004; 45:465–476. [PubMed: 15822185]
38. Moreau P, Richardson PG, Cavo M, Orlowski RZ, San Miguel JF, Palumbo A, et al. Proteasome inhibitors in multiple myeloma: 10 years later. Blood. 2012; 120:947–959. [PubMed: 22645181]
39. Yu X, Patterson E, Kem DC. Targeting proteasomes for cardioprotection. Curr Opin Pharmacol. 2009; 9:167–172. [PubMed: 19097937]
40. Bockorny M, Chakravarty S, Schulman P, Bockorny B, Bona R. Severe heart failure after Bortezomib treatment in a patient with multiple myeloma: a case report and review of the literature. Acta Haematol. 2012; 128:244–247. [PubMed: 22964848]
41. Day SM. The ubiquitin proteasome system in human cardiomyopathies and heart failure. Am J Physiol Heart Circ Physiol. 2014; 304:H1283–H1293. [PubMed: 23479263]
42. Pagan J, Seto T, Pagano M, Cittadini A. Role of the ubiquitin proteasome system in the heart. Circ Res. 2013; 112:1046–1058. [PubMed: 23538275]
43. Leykauf K, Salek M, Bomke J, Frech M, Lehmann WD, Durst M, et al. Ubiquitin protein ligase Nedd4 binds to connexin43 by a phosphorylation-modulated process. J Cell Sci. 2006; 119:3634–3642. [PubMed: 16931598]
44. Li X, Su V, Kurata WE, Jin C, Lau AF. A novel connexin43-interacting protein, CIP75, which belongs to the UbL-UBA protein family, regulates the turnover of connexin43. J Biol Chem. 2008; 283:5748–5759. [PubMed: 18079109]
45. Das S, Smith TD, Sarma JD, Ritzenthaler JD, Maza J, Kaplan BE, et al. ERp29 restricts Connexin43 oligomerization in the endoplasmic reticulum. Mol Biol Cell. 2009; 20:2593–2604. [PubMed: 19321666]
46. Arora A, Minogue PJ, Liu X, Reddy MA, Ainsworth JR, Bhattacharya SS, et al. A novel *GJA8* mutation is associated with autosomal dominant lamellar pulverulent cataract: further evidence for gap junction dysfunction in human cataract. J Med Genet. 2006; 43:e2. [PubMed: 16397066]
47. Laing JG, Tadros PN, Green K, Saffitz JE, Beyer EC. Proteolysis of connexin43-containing gap junctions in normal and heat-stressed cardiac myocytes. Cardiovasc Res. 1998; 38:711–718. [PubMed: 9747439]

## Highlights

- We studied connexin40 mutants linked to atrial fibrillation.
- Several mutants (including G38D) exhibited minimally altered conductance and gating properties.
- In contrast, they showed accelerated degradation.
- G38D levels and function were restored by treatment with the proteasomal inhibitor, epoxomicin.
- Proteasomal inhibition might be a novel therapy for arrhythmias caused by some connexin mutants.

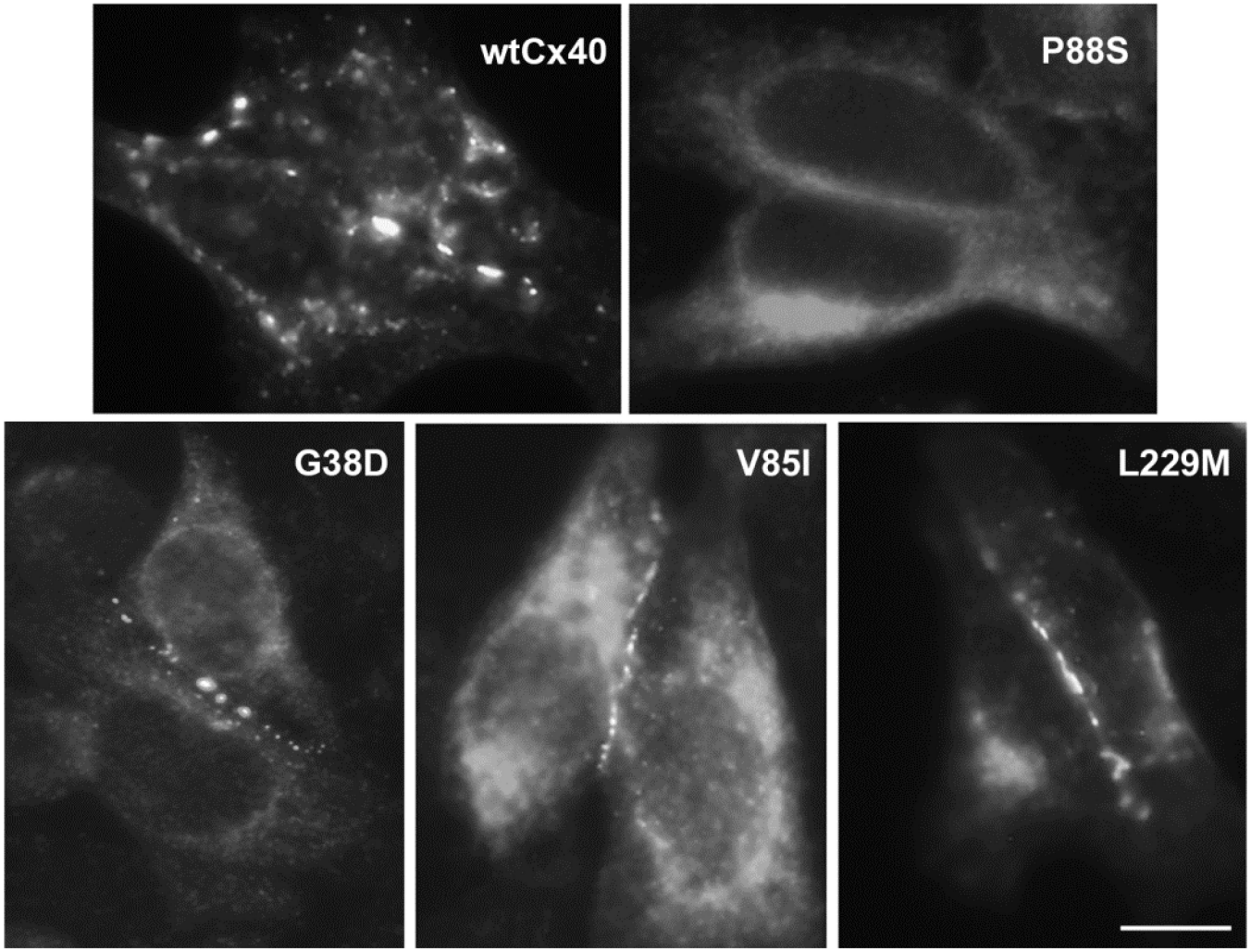


**Figure 1. Many, but not all, AF-associated Cx40 mutants make gap junctions when expressed in communication-deficient cells**

Wild type Cx40 or AF-associated mutants (G38D, V85I, P88S, and L229M) were detected by immunofluorescent localization in transiently transfected HeLa cells. Wild type Cx40 and most of the mutants, including G38D, V85I, and L229M, were localized in a punctuate distribution along appositional membranes within the cytoplasm. P88S was retained intracellularly. Bar, 10 μm.

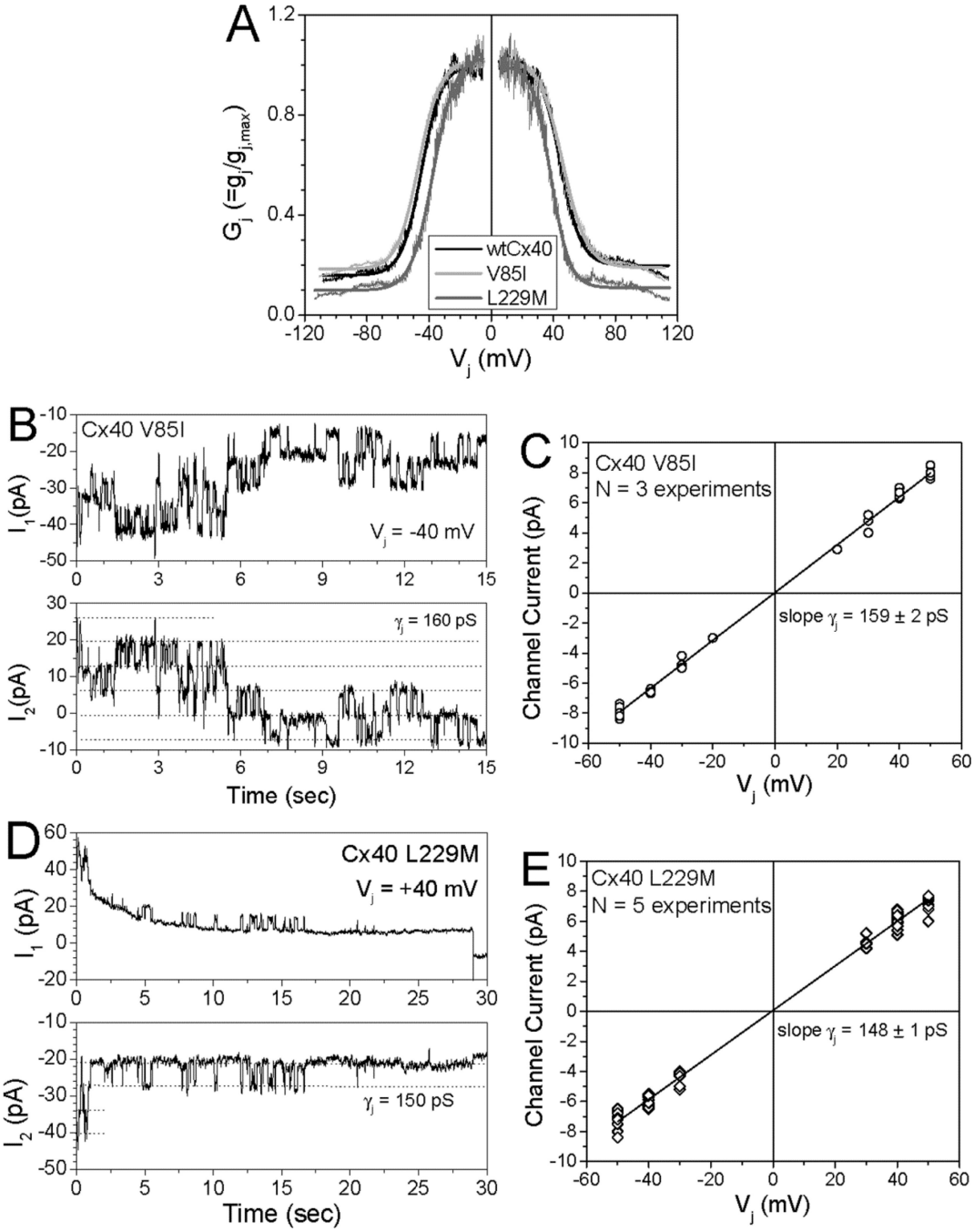


**Figure 2. Gap junction channels formed by V85I or L229M had normal or mildly altered Vj-dependent gating and single channel conductances**

**(A)** Plots show the relationships between normalized junctional conductance ($G_j$) and transjunctional voltage ($V_j$) for homomericwtCx40 (black), V85I (light gray) and L229M (dark gray) gap junctions. The Boltzmann parameters for the fitted curves are listed in Supplemental Table 1 **(B)** Whole cell currents ($I_1$ and $I_2$) were recorded simultaneously for 15 sec. from a pair of N2a cells expressing V85I during a 40 mV $V_j$ step applied to cell 1. Current amplitudes are indicated by dashed lines in the $I_2$ trace ($I_j = -\Delta I_2$). **(C)** Junctional

current-voltage ($I_j$–$V_j$) relationship for V85I channels was generated from channel current amplitudes determined by Gaussian fits of the all points current histogram (not shown) for each 30 s $V_j$ pulse. The mean slope conductance ($\gamma_j$) was 159 ± 2 pS. **(D)** Whole cell currents are shown for a 30 sec. recording of a L229M channel during a +40 mV $V_j$ pulse. **(E)** The $I_j$−$V_j$ relationship for L229M is shown. The mean slope $\gamma_j$ was 148 ± 2 pS.

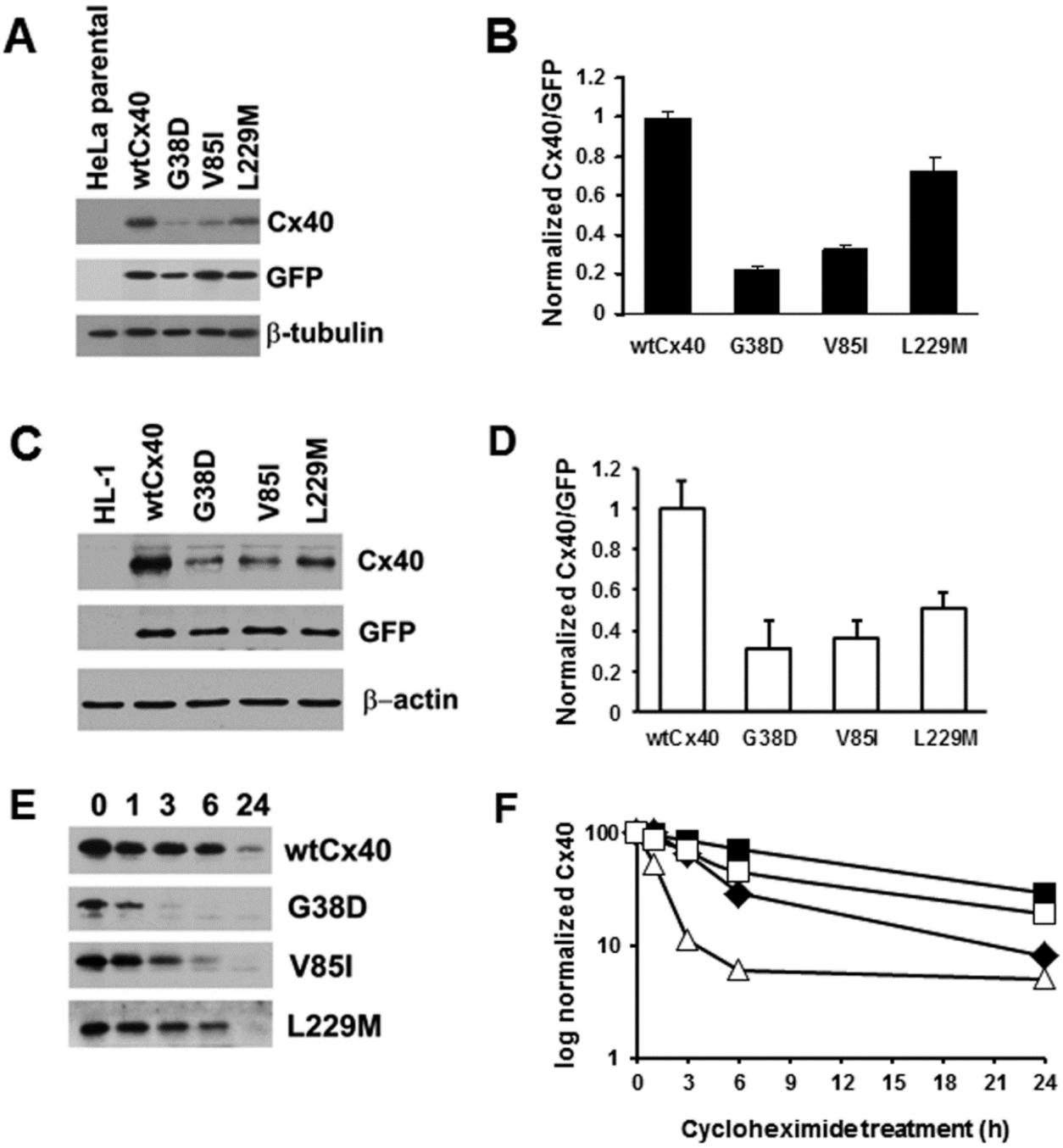


**Figure 3. Several mutants show reduced Cx40 levels and faster degradation than wild type Cx40**

**(A)** Immunoblot of wtCx40 and Cx40 mutants expressed in HeLa cells. Lysates were prepared from (untransfected) HeLa cells and HeLa cells transiently transfected with Cx40 or AF mutants (in pTracer-CMV2) and subjected to immunoblotting using antibodies directed Cx40, GFP (to establish the efficiency of transfection) and β-tubulin (as a loading control). The identical blots were used for probing with each of the different antibodies after stripping. Representative lanes were cropped from a larger blot. **(B)** Graph shows levels of wtCx40 and mutants. The Cx40 and GFP bands were analyzed by densitometry for each

construct. The ratio of Cx40:GFP was calculated for each construct (to correct for any differing efficiencies of transfection). Levels of expression were compared to the wtCx40. Values represent the mean +SEM, n=3. Levels of G38D, V85I, and L229M were all statistically different from wild type (Student's t-test, $p<0.05$). **(C)** Immunoblot of wtCx40 and Cx40 mutants expressed in HL-1 cells. Lysates were prepared from (untransfected) HL-1 cells and HL-1 cells transiently transfected with Cx40 or AF mutants (in pTracer-CMV2) and subjected to immunoblotting using antibodies directed against Cx40, GFP (to establish the efficiency of transfection) and β-actin (as a loading control). The identical blots were used for probing with each of the different antibodies after stripping. **(D)** Graph shows levels of wtCx40 and mutants expressed in HL-1 cells. Densitometry was performed as described for panel B. Values represent the mean +SEM, n=3. Levels of G38D, V85I, and L229M were all statistically different from wild type (Student's t-test, $p<0.05$). **(E)** Immunoblot analysis of HeLa cells transfected with wild type or mutant Cx40 and then treated with cycloheximide for 0, 1, 3, 6 or 24 h. (**F**) Graphs shows the levels of immunoreactiveCx40 (wild type or mutants) at different intervals of treatment with cycloheximide (based on quantification of the immunoblots). Values derive from analysis of the Cx40 bands by densitometry and normalization of the abundance at each time point to the abundance at time 0.

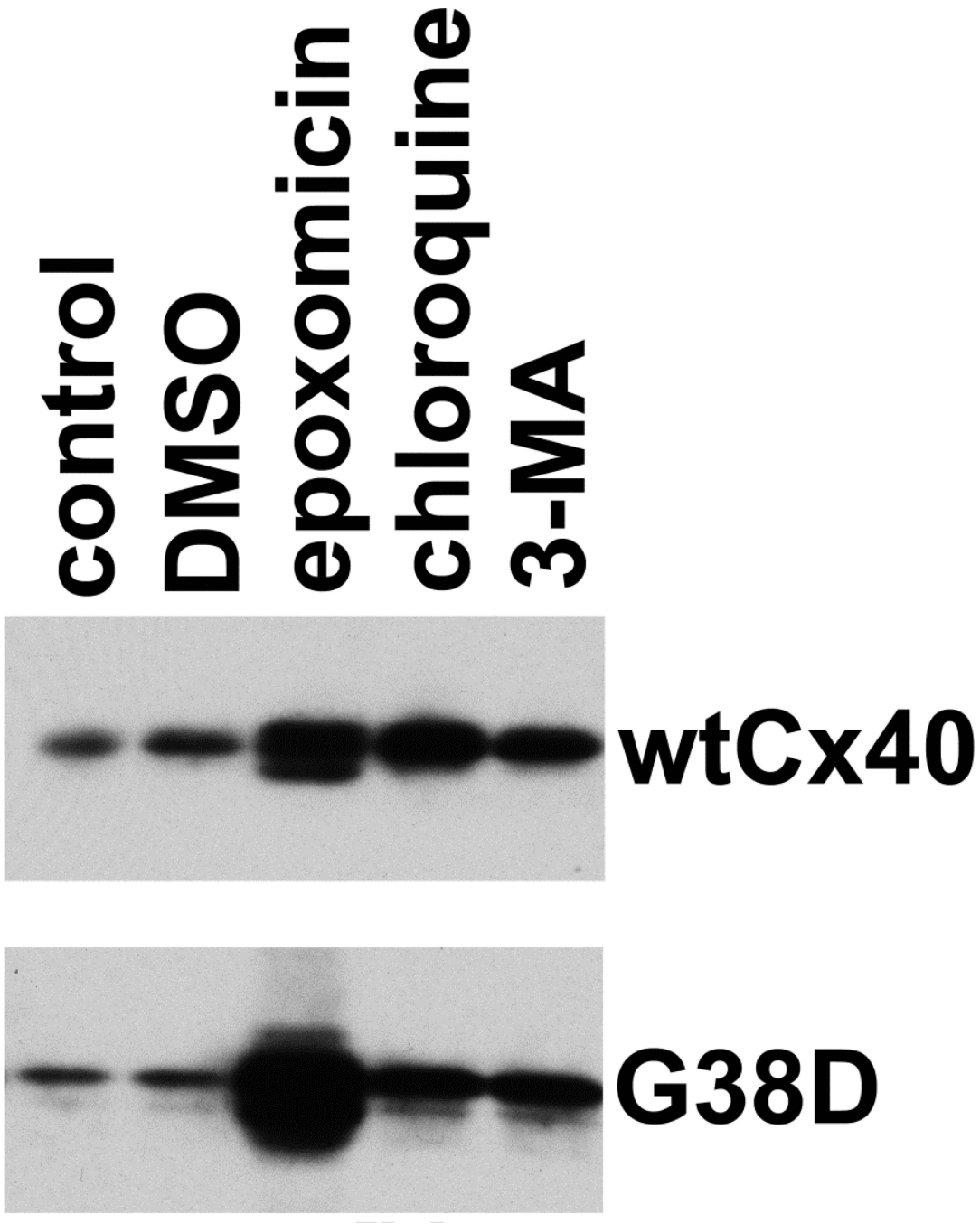


**Figure 4. The proteasomal inhibitor, epoxomicin, blocks the accelerated degradation of G38D**

HeLa cells were transiently transfected with wtCx40 or G38D, and 48 h later were treated for 18 hours with chloroquine (to inhibit the lysosome), 3-methyl adenine (3-MA; to inhibit autophagy) or epoxomicin (to block the proteasome). The cells were harvested and analyzed by immunoblotting to determine levels of immunoreactive Cx40. Although each of the drugs produced an increase in both wtCx40 and G38D, the relative increase for G38D was much greater following epoxomicin, implicating the proteasome in the accelerated degradation of this mutant.

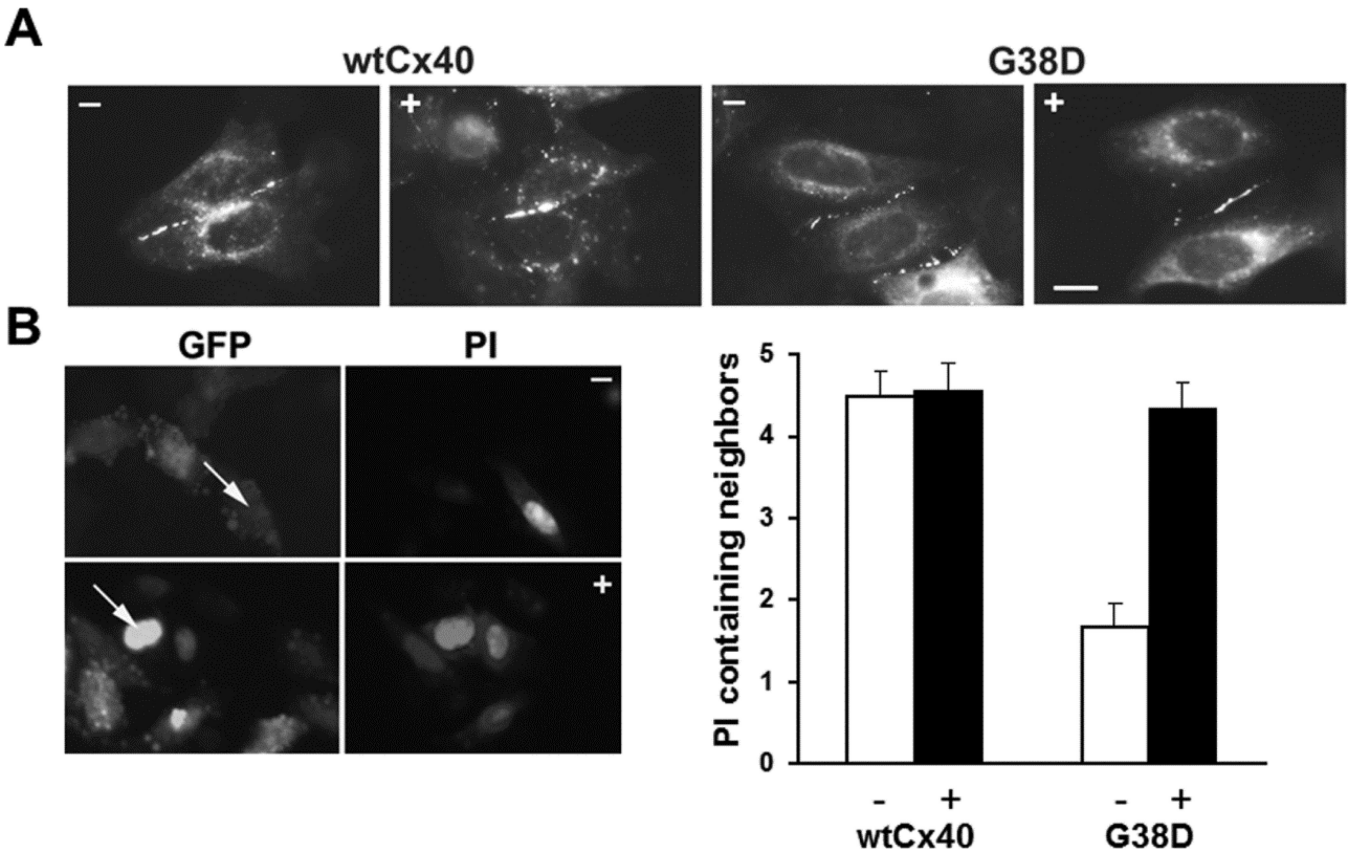


**Figure 5. The proteasomal inhibitor, epoxomicin also increases gap junction size/abundance and intercellular communication in HeLa cells expressing G38D**

**(A)** Photomicrographs show immunofluorescent detection of the distributions of Cx40 in HeLa cells transiently transfected with wtCx40 or G38D. Cells were untreated (−) or exposed to 0.5μM epoxomicin (+) for 4 hours. Bar, 10 μm. **(B)** Photomicrographs show examples of the intercellular transfer of microinjected PI between HeLa cells transiently transfected with G38D. Cells were untreated (−) or exposed to 0.5μM epoxomicin (+) for 4 hours. GFP fluorescence (also expressed from the pTracer plasmid) allowed identification of the transfected cells. Arrows show injected cells. The bar graph shows the extent of dye transfer (PI containing neighbors) after injection of that tracer in cells transfected with wtCx40 or G38D. Cultures were untreated (−, white bars) or treated with 0.5μM epoxomicin (+, black bars).The extent of transfer was not statistically different between control wtCx40-expressing cells and those treated with epoxomicin. In HeLa cells transfected with G38D, transfer of PI was dramatically increased after epoxomicin treatment as compared to vehicle –treated control cultures ($p<0.001$). Epoxomicin treatment increased dye transfer in G38D–expresssing cells to levels comparable to those in cells expressing wtCx40. Values represent the mean + SEM, n=9−29.

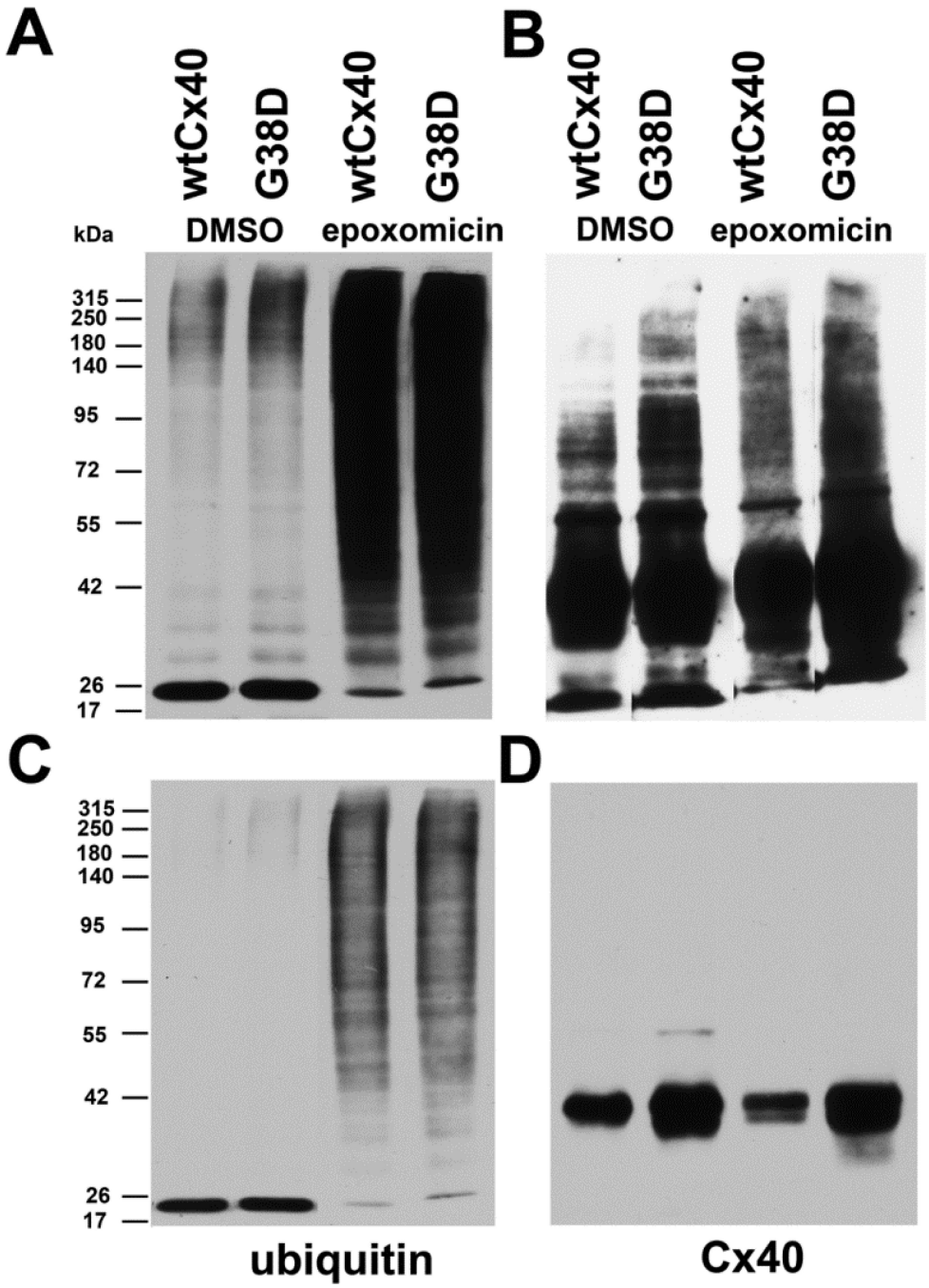


**Figure 6. Wild type Cx40 and G38D are ubiquitinated**

HeLa cells stably transfected with wtCx40 or G38D were treated with DMSO (control) or with 0.5μM epoxomicin for 18h. Ubiquitinated proteins were isolated from cell lysates and analyzed by immunoblotting with antibodies directed against ubiquitin **(A,C)** or Cx40 **(B,D)**. The same blot was probed sequentially with both antibodies with intervening stripping . Eluates equivalent to 10μg of total protein in the starting lysate were loaded in each lane. Top panels **(A, B)** show long exposures and bottom panels **(C,D)** show shorter exposures of the same blots. Epoxomicin increased the abundance of ubiquitinated proteins

**(A,C)** in cells expressing either wtCx40 or G38D. Immunoreactive Cx40 was isolated with the ubiquitinated proteins from both cell lines (**B,D**), and the abundance of slower migrating forms (likely polyubiquitinated Cx40) was increased following epoxomicin treatment **(B)**.

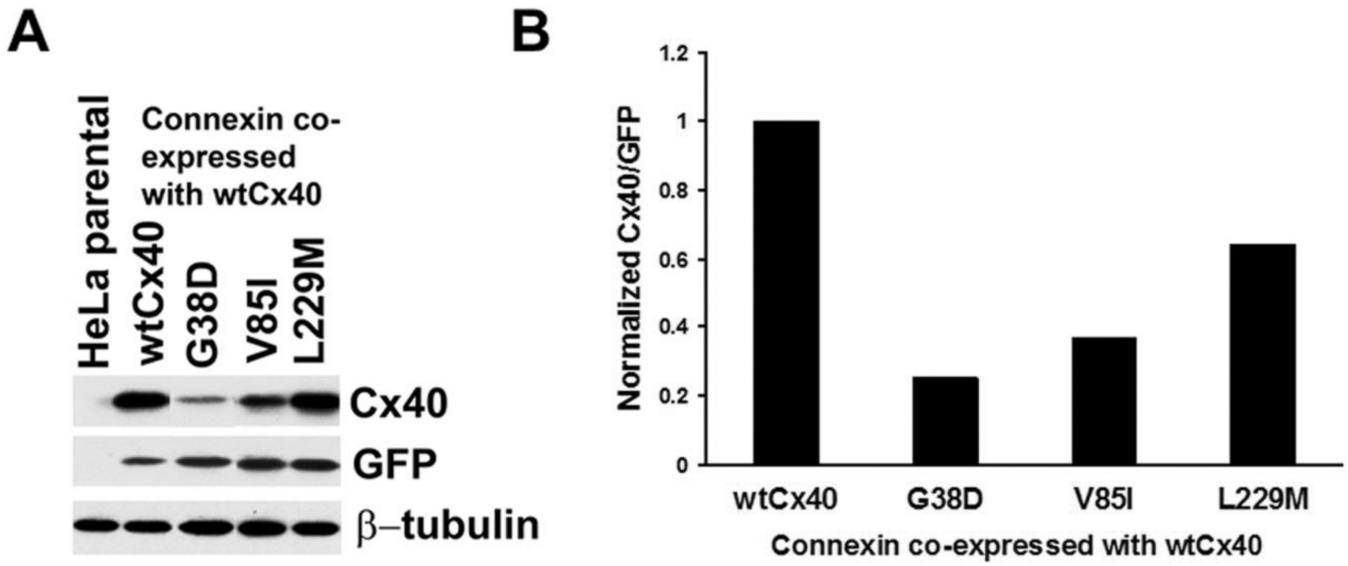


**Figure 7. AF Cx40 mutants reduce total Cx40 levels when co-expressed with wild type Cx40**

HeLa cells were transiently co-transfected with a plasmid encoding wild type Cx40 and an equal amount of plasmid encoding wild type or mutant Cx40. **(A)** Levels of total immunoreactive Cx40 were detected by immunoblotting. Blots were also probed with antibodies directed against GFP (transfection efficiency control) and β-tubulin (loading control). Although this experiment was performed in duplicate, some lanes were eliminated to include only representative examples. **(B)**. Graph shows the total amounts of immunoreactive Cx40 (includes wild type and mutant) for cells transfected with wtCx40 plus wild type or mutant Cx40. Values were normalized according to the densities of the GFP bands and averaged from duplicates. Cx40 levels are lower in cells transfected with each of the mutants (and most severely reduced for G38D) suggesting that they also accelerate the degradation of the wild type protein.

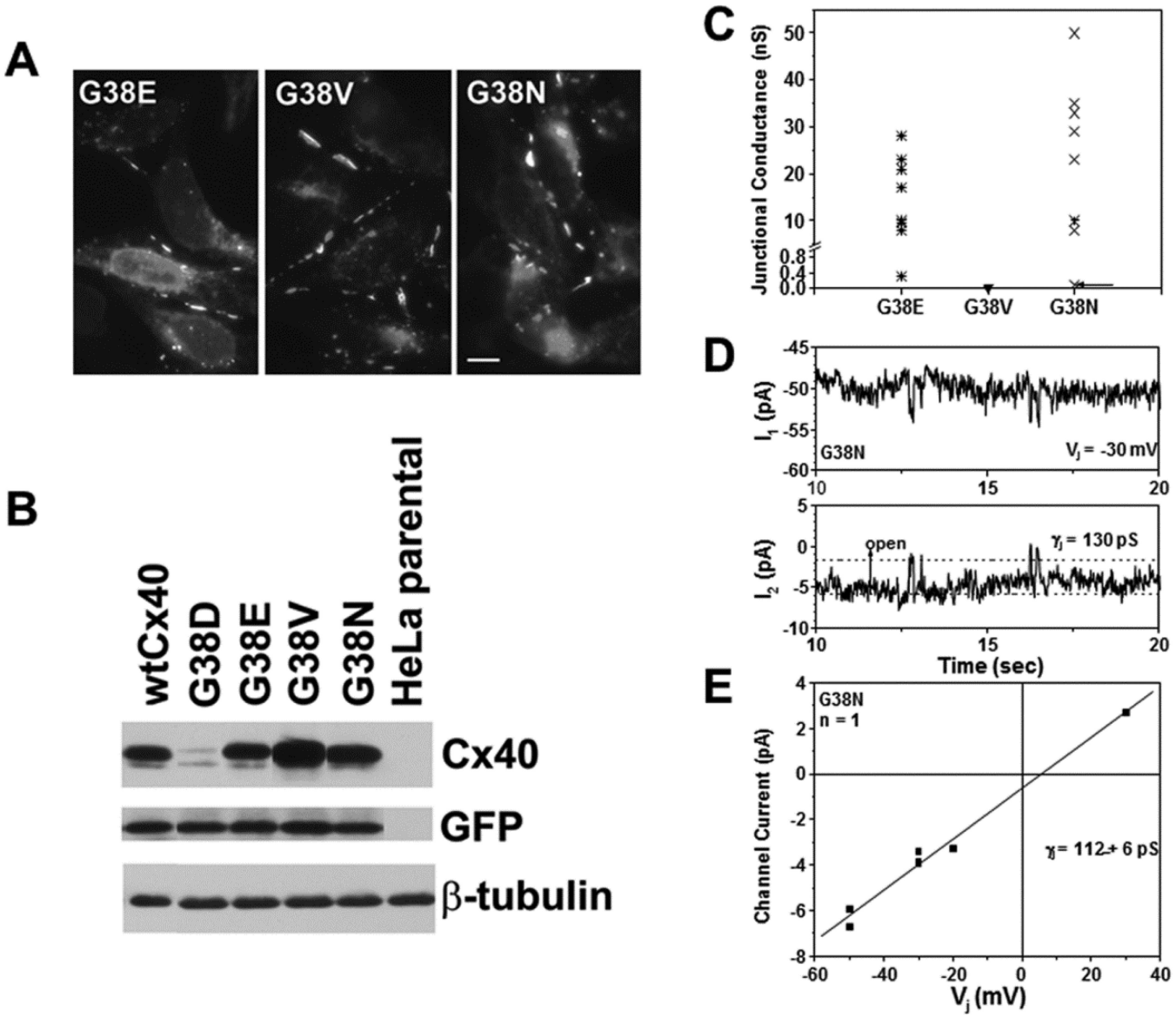


**Figure 8. While all site directed mutants at position G38 form gap junction plaques and differ in channel properties, only G38D has reduced protein levels as compared to wild type Cx40**

**(A)** Immunofluorescent detection of the distributions of immunoreactiveCx40 in HeLa cells transiently transfected with G38E, G38V, or G38N. Each of these mutants localizes to appositional plasma membranes. Bar, 10 μm. **(B)** Immunoblot detection of Cx40 in untransfected HeLa cells or cells that were transiently transfected wtCx40, G38D, G38E, G38V, or G38N. Although this experiment was performed in triplicate, some lanes were eliminated to illustrate only representative examples. Blots were also probed with antibodies directed against GFP (transfection efficiency control) and β-tubulin (loading control). Only G38D shows reduced levels as compared to wtCx40. **(C)** Graph shows total junctional conductance in pairs of cells transiently transfected with G38E, G38V, or G38N. While both G38E and G38N formed large conductances in all cell pairs studied, gap junctional coupling was not detected in cell pairs expressing G38V. **(D)** Tracings show single channel events

recorded from an N2a cell pair expressing G38N. Whole cell currents ($I_1$ and $I_2$) were recorded simultaneously for 10 sec. during a 30 mV $V_j$ step applied to cell 1. **(E)** Junctional current-voltage ($I_j$ –$V_j$) relationship for G38N channels was generated from channel current amplitudes determined by Gaussian fits of the all points current histogram. The mean slope conductance ($\gamma_j$) was 112 ± 6pS.